Network Pharmacology Prediction and Molecular Docking-Based Strategy to Discover the Potential Pharmacological Mechanism of Wen-yu-jin Against Pulmonary Fibrosis in Mouse Model

lu wang
Beijing University of Chinese Medicine https://orcid.org/0000-0001-5244-2263
Wenxiang Zhu
Beijing University of Chinese Medicine
Rui Sun
Beijing University of Chinese Medicine
Jing Liu
Beijing University of Chinese Medicine
Qihong Ma
Beijing University of Chinese Medicine
Binbin Zhang
Beijing University of Chinese Medicine
Yuanyuan Shi (yshi@bucm.edu.cn)
Beijing University of Chinese Medicine https://orcid.org/0000-0003-2997-4573

Research

Keywords: wen-yu-jin (WYJ), lung fibrosis, network pharmacology, molecular docking, MAPK signaling pathway, STAT3

Posted Date: October 12th, 2021

DOI: https://doi.org/10.21203/rs.3.rs-923117/v1

Version of Record: A version of this preprint was published at Evidence-Based Complementary and Alternative Medicine on February 10th, 2022. See the published version at https://doi.org/10.1155/2022/7753508.

Abstract

Background

Pulmonary fibrosis (PF) is a devastating lung disease. The two drugs approved by the FDA, pirfenidone and nintedanib, can only delay the progression of the disease but cannot cure the disease. These drugs also present adverse effects. Wen-yu-jin (WYJ) obtained from steamed roots of Curcuma wenyujin showed a variety of pharmacological activities. In this study we investigated whether WYJ present anti-lung fibrosis effects.

Methods

Ultra-high pressure liquid chromatography combined with linear ion trap-orbital tandem mass spectrometry (UHPLC-LTQ-orbital trap) was used to identify chemical composition of WYJ. PF-related and WYJ-related targets were obtained from public databases. Network pharmacological was performed to acquire potential targets and major signaling pathways. The binding activity of composition with core targets was predicted by molecular docking. Based on the predicted results, the anti-lung fibrosis effect of WYJ was verified in vivo and in vitro experiments.

Results

23 major compositions of WYJ were identified based on UHPLC-LTQ-Orbitrap. According to the results of network pharmacology, MAPK signaling pathway might play an important role in WYJ against lung fibrosis and STAT3 also could be the potential therapeutic targets. Molecular docking results indicated that most of the compositions have good binding activities with core targets. In vivo and in vitro experiments showed that WYJ alleviated process of fibrosis by inhibiting MAPK signaling pathway and the levels of phosphorylated STAT3 (p-STAT3).

Conclusion

According to the results of network pharmacology and molecular docking, in vivo and in vitro experiments further verified potential targets and molecular mechanism of WYJ against lung fibrosis. Our study provided a novel approach to explain the pharmacological basis of other herbs.

Introduction

PF characterized by bilateral pulmonary interstitial infiltration, restriction on pulmonary function testing, and progressive dyspnea with respiratory failure[1–3], is an irreversible lung disease[4]. Idiopathic pulmonary fibrosis (IPF) is the most common type of pulmonary fibrosis. PF susceptibility is closely related to aging, which leads to telomeres shortening and mitochondrial dysfunction[5]. Accumulating exposures to numerous risk factors[6] such as smoking, occupational dust, drug stimulation, bacterial and virus infection, also result in PF. Pirfenidone and nintedanib[7, 8] approved by FDA are the only two effective drugs for clinical PF medical therapies. However, these drugs only can delay the progression of the disease and maintain lung function but cannot cure the disease[9, 10]. And these drugs can cause adverse effects[10–12], resulting in treatment discontinuation and adverse gastrointestinal effects.

Multiple active ingredients and targets of Traditional Chinese Medicines (TCMs) arouse the attention of pharmacologists. Previous studies showed that TCMs or active ingredients from TCMs have pulmonic protective benefits[13], which represent an attractive source of drug discovery for treating PF. In TCMs, there are many theories according to the pathogenesis of PF, such as qi stagnation and blood stasis (Qi-Zhi-Xue-Yu in Chinese) and binding of phlegm and qi (Tan-Qi-Hu-Jie in Chinese). Wen-yu-jin (WYJ, Curcuma Radix, □□□), derived from the steamed root of Curcuma wenyujin, has been used for at least 1500 years in China and was mainly dependent on move qi and activate blood to intervene diseases.

In our study, a novel approach combining TCMs with network pharmacology was established to explore the molecular mechanism of WYJ against PF. Molecular docking was performed to predict the affinity strength between the active Compounds and the important targets. Finally, the anti-fibrosis mechanism of WYJ was further verified via in vitro and in vivo experiments based on the predicted results.

Materials And Methods

Preparation of Chinese Medicine

WYJ was purchased from Tong Ren Tang Co., Ltd. (Beijing, China). The herb was boiled in purified water twice for 1h each time. Lyophilized powder was obtained by condensation and freeze-dry of liquids. Lyophilized powder was stored at -80℃ and used for a series of experiments.

LC/MS Analysis

The coupling of UHPLC System (Thermo Fisher Scientific) equipped with a binary pump, an autosampler, a column thermostat and DAD detector and LTQ-Orbitrap XL (Thermo Fisher Scientific) equipped with an electrospray ionization source (ESI) was used For LC/MS experiments. Data was controlled and processed by Xcalibur software (Thermo Fisher Scientific). The column used in the LC analysis was Thermo Scientific Hypersil BDS C18

(2.1mm × 150mm,2.4 μm). Mobile phase A was water with 0.1% formic acid while mobile phase B is acetonitrile. The column temperature was set to 35℃ and the flow rate was 0.3mL/min. Elution conditions were summarized as follows: 0-3min (5%-5%B), 3-45min (5%~75%B)，45-45.1min (75%-5%B), 45.1-50min (5%-5%B).

The MS analysis was conducted on both the negative and positive ion modes. Flow rates of sheath gas and auxiliary gas were set at 40 Arb and 20 Arb, respectively. The capillary voltage was set to 35.0 V, the source temperature was set to 350 ℃ and the tube lens was set to 110 V. The source voltage was set to 4 KV and 3 KV in the positive and negative ion modes respectively.

Network Pharmacology

According to the Compounds identified by UHPLC-LTQ-Orbitrap, WYJ-related targets were obtained from SwissTargetPrediction database[14] (http://www.swisstargetprediction.ch/) and Traditional Chinese Medicine Systems Pharmacology Database and Analysis Platform (TCMSP, https://tcmsp-e.com/). The SDF format file of each Compound structure was obtained from PubChem database (https://pubchem.ncbi.nlm.nih.gov/) and loaded into the SwissTargetPrediction database to predict the targets. Compounds-related protein names obtained from TCMSP need converting to the gene names using UniProt (https://www.uniprot.org/). Combined with the results of the two databases, the targets of WYJ were obtained.

PF-related targets were obtained from GeneCards database v5.0[15] (https://www.genecards.org/, Relevance score ≥ median values) and OMIM database[16] (https://omim.org/) using “pulmonary fibrosis (PF)”, “idiopathic pulmonary fibrosis (IPF)” or “interstitial lung disease (ILD)” as the keywords. After combining the targets obtained from different databases using the same keywords, the intersection of the targets from different keywords were the targets of PF.

WYJ-related targets and PF-related targets were intersected to obtain gene symbols. Using STRING database (https://www.string-db.org/)[17],the protein-protein interaction (PPI) network was constructed to explore the potential interactions of the intersected gene symbols. Cytoscape v3.6.0 visualized PPI network. Critical nodes calculated by median values of three topological features (degree, closeness centrality, and betweenness centrality) were identified as the key targets of WYJ.

To determine biological meaning behind key targets, pathway enrichment was analyzed by Gene Ontology (GO) and Kyoto Encyclopedia of Genes and Genomes (KEGG) databases in DAVID v6.8 (https://david.ncifcrf.gov/)[18, 19].The threshold value of confident gene enrichment was set at P＜0.05. Compound–target-pathway network explored the connections of compounds of WYJ, key targets, and important signaling pathways and was visualized using Cytoscape.

Molecular Docking

Based on results of LC/MS analysis and network pharmacology, we downloaded the 2D structures of ligands from PubChem database and the structures of target proteins from the PDB (https://www1.rcsb.org/). MGLTool-1.5.6 was used for generating necessary pdbqt file format of proteins and ligands along with the respective grids and dock files. AutoGrid 4.2 and Auto vina[20] were adopted to generate grids and execute docking respectively. 10 different conformations of each protein and compound were obtained and analyzed. PyMOL’s visualization property[21] was used for the image construction of the docked ligand protein complexes. The binding affinities of the complexes were recorded in the log files of the docks generated by Auto vina.

Experimental Verification

Animals and experimental design

75 male mice (18-22g, 8 weeks old) were purchased from Beijing Vital River Laboratory Animal Technology Co., Ltd. (Beijing, China). The mice were anesthetized to reduce pain in the procedures. Mice of the Control group were given normal saline via oropharynx, and other mice were given bleomycin (BLM) via oropharynx at a dose of 5 mg/kg to establish PF model. BLM-induced PF model were randomly divided into four groups: BLM treatment group (Model); BLM with WYJ high concentration treatment group (WYJ-H); BLM with WYJ medium concentration treatment group (WYJ-M); and BLM with WYJ low concentration treatment group (WYJ-L).

Control group and Model group were treated with saline. According to the previous reports and the results of pre-experiments, WYJ-H, WYJ-M and WYJ-L groups were given WYJ at doses of 1.2, 0.6, and 0.3g/kg respectively. All the treatments were initiated 7 days after the establishment of PF model with bleomycin, once a day for 14 days. All the mice were sacrificed on day 22. Lung tissue was stored at -80℃ for different experiments.

Lung/Body Weight Ratio

The body weight (BW) and the whole lung weight (PW) were recorded after mice were sacrificed. Pulmonary indexes (PI) were calculated using the equation PI = PW/BW*100.

Hydroxyproline determination (HYP)

The lung tissue was processed according to the instructions of the Hydroxyproline Kit (Nanjing Jiancheng Institute of Bioengineering, Nanjing, China). The level of hydroxyproline in the lung tissue was measured at the absorbance of 550nm and the results were expressed with μg/ lung.

Histopathological examination

Lung tissues fixed with 10% formalin were embedded in paraffin and sectioned. Sections were stained with hematoxylin-eosin (H&E) and Masson. Experienced pathologists performed sections pathological evaluation under light microscopy.

Culture of human pulmonary fibroblast(HPF)

HPF, a normal human fibroblast cell line from the National Infrastructure of Cell Line Resource (Beijing, China). HPF were cultured in medium (DMEM) with 10% FBS and 1% PS and maintained at the cell incubator with 5% CO2 and 37℃. Cells were passaged at a confluence of 80%-90% by standard trypsinization techniques. HPF stimulated with TGF-β1 (10ng/mL) were compared with cells that grown in the same conditions, but without stimulation of TGF-β1.

Cell viability analysis

The viability of HPF treated with WYJ was assessed using CCK-8 (CK001, Lablead). Firstly, HPF were seeded into 96-well plate in the density of 2×104 cells/well and treated with or without WYJ (0, 0.1, 1, 10, 20 or 50μg/mL) after 12-24h. Secondly, each well was added 200μL medium with 10% CCK-8 solution after 48h and then incubated at 37℃ for 1-2h. Finally, the absorbance of well was measured at 490 nm using a microplate reader (Molecular Devices, Sunnyvale, CA, USA).

Quantitative real-time polymerase chain reaction (qPT-PCR)

Total RNA extracted from HPF or mouse lung tissues using Trizol reagent (Qiagen, New York, USA) was purified with RNeasy column (Qiagen, New York, USA). cDNA was obtained from purified RNA using a reverse transcription Kit (Qiagen, New York, USA) following manufacturer's instructions. Making full use of QuantStudio6 Flex, gene expression analysis was performed following instructions of QuantiFast SYBR Green PCR kit (Qiagen, New York, USA). Fold changes of relative gene expression were calculated using the 2-△△Ct method. Gene primer sequences are shown in Table 1.

Table 1
Gene Primer Sequences

Gene		Primer(5'-3')	Accession no.
Mus -GAPDH	Forward	AGGTTGTCTCCTGCGACTTCA	NM_008084.3
	Reverse	TGGTCCAGGGTTTCTTACTCC	
Mus -Col1a1	Forward	CCAAGAAGACATCCCTGAAGTCA	NM_007742.4
	Reverse	TGCACGTCATCGCACACA	
Mus -TGF-β1	Forward	ATGACATGAACCGGCCCTT	NM_011577.2
	Reverse	AGTTGGTATCCAGGGCTCTCC	

Western blotting

Proteins obtained from lung tissue or cells were further analyzed with Bicinchoninic Acid (Applygen, Beijing, China)for protein concentration. Protein at 30–50 μg/lane was loaded and separated by SDS-PAGE gel electrophoresis. After SDS-PAGE, proteins were transferred to the Polyvinylidene Fluoride (PVDF) membranes (Millipore, Massachusetts, USA). Membranes were blocked in 5% fat-free milk dissolved with Tris-buffered saline with Tween 20 (TBST) for 120 min at room temperature. Rinsed with TBST, these membranes incubated with primary antibodies at 4℃ overnight. On the second day, the blots were rinsed with TBST and then incubated with secondary antibody for 1h. Blots were visualized by gel imager. GAPDH was used loading positive control and the results were analysed using image J.

Antibodies: Anti-α-SMA (ab5694, abcam, Cambridge, UK), Anti-Collagen 1 (14695, Proteintech), anti-p-MAPK (ab201015, abcam), anti-MAPK (ab184699, abcam), anti-p-STAT3 (ab76315, abcam), anti-STAT3 (ab68153, abcam), anti-GAPDH (60004, Proteintech, Chicago, USA), anti-rabbit IgG (ab205718, abcam) and anti-mouse IgG (ab6728, abcam).

Data and statistical analysis

One-way ANOVA were performed using GraphPad Prism software (version 8.0.2). P values < 0.05 are adopted as statistically significant.

Results

Identified Ingredients of WYJ

Using UHPLC-LTQ-Orbitrap to detect and identify chemical Compounds of WYJ (Fig. 1), a total of 23 compounds were confirmed based on comprising with the published data. Information about the identified ingredients was summarized in Tables 2 and 3.

Table 2
Chemical Compositions of WYJ in Negative Ion Mode

NO.	tR/min	Molecular formula	Accurate mass[M – H]-	Calculated mass[M – H]-	Fragmentation(MS/MS)	Error (ppm)	Identified compounds	PubChem CID
1	11.58	C10H10O3	177.0552	177.0555	162.0325;113.002;92.9957	1.694	(Z)-p-Methoxycinnamic acid	1550936
2	18.13	C15H18O3	245.1178	245.1186	180.9893;175.0763;57.0345	3.264	Curcolone	12304272
3	21.68	C15H18O3	245.1178	245.1182	224.9971;201.1285;180.9894	1.632	Zedoarol	46173920
4	27.14	C15H20O3	247.1334	247.1339	229.1234;203.1078;189.0921;161.0971	2.023	Curcumenolactone A	10083354
5	25.28	C15H22O3	249.1491	249.1497	228.9897;205.1598;154.9738;112.9857	2.408	procurcumadiol	14633012
6	25.29	C15H24O3	251.1647	251.1654	207.1753;191.1442;125.0972;57.0346	2.787	zedoarondiol	24834047
7	22.62	C15H22O4	265.144	265.1445	194.9886;112.9856;68.9957	1.886	Zedoalactone A	15226639
8	19.77	C15H12O5	271.0607	271.0613	186.9991;151.0036;119.0501	2.214	naringenin	439246
9	11.56	C15H20O5	279.1233	279.1236	235.1339;217.1232;181.0869;137.097	1.075	Zedoalactone B	15226640
10	24.88	C21H22O6	369.1338	369.1347	354.1110;247.0974;218.0585;140.0114	2.438	1,2-Dihydrocurcumin	5372374

Table 3
Chemical Compositions of WYJ in Negative Ion Mode

NO.	tR/min	Molecular formula	Accurate mass[M + H]+	Calculated mass[M + H]+	Fragmentation(MS/MS)	Error (ppm)	Identified compounds	PubChem CID
11	17.67	C10H12O	149.0966	149.0962	121.0649	-2.683	cuminal	326
12	18.02	C19H16O4	309.1127	309.1111	281.0920;62.9826	-5.176	bisdemethoxycurcumin	45934475
13	24.07	C15H20	201.1643	201.1638	169.0860;141.091;113.0601	-2.486	calacorene	12302243
14	45.72	C15H22	203.18	203.1796	175.1482;133.1013;109.1016;81.0706	-1.969	(+)-alpha-Curcumene	3083834
15	30.43	C15H16O	213.1279	213.1275	195.1169;157.1013	-1.877	Pyrocurzerenone	12314812
16	32.49	C15H20O	217.1592	217.1588	161.0961;137.0961;95.0860;	-1.842	ar-turmerone	160512
17	31	C15H16O2	229.1228	229.1223	NA	-2.182	Gweicurculactone	130117
18	34.07	C15H18O2	231.1385	231.1381	213.1275;173.0962;85.0653	-1.731	Epicurzerenone	5317062
19	15.7	C15H20O2	233.1541	233.1536	215.1432;187.1482;175.1118	-2.145	Furanogermenone	6439596
20	24.49	C15H20O2	233.1541	233.154	NA	-0.429	turmeronol A	15858385
21	15.39	C15H22O2	235.1698	235.1692	217.1587;189.1638;135.1169;97.0653	-2.551	germacrone-13-al	46173921
22	19.31	C15H24O2	237.1854	237.1847	219.1381;173.1362;133.1013	-2.951	Curcumalactone	15071433
23	16.39	C15H20O3	249.149	249.1485	231.1379	-2.007	Curcumenolactone B	10264037

Network and Pathway Analysis

Based on methods above, 436 WYJ-related targets were obtained from SwissTargetPrediction and TCMSP after removing duplicate items. Information about WYJ-related targets was provided in Supplementary Table S1. Combining the search results of the same keyword from GeneCards and OMIM database,a total of 2,867 targets for PF, 1,287 targets for IPF and 1,613 targets for ILD were collected. As shown in Fig. 2A, 846 overlapping targets were considered to be important targets about PF. The details were shown in Supplementary Table S2. Combining 463 WYJ-related targets with 846 PF-related targets, 124 targets could be the potential targets for the WYJ treatment on PF (Fig. 2B). Detailed information about 124 potential targets was provided in Supplementary Table S3.

STRING databases were used to explore the underlying interactions of 124 potential targets. There were 124 nodes and 1716 edges in the PPI network visualized by Cytoscape (Fig. 3). According to the conditions of three topological (degree≥22, betweenness centrality≥0.00208, and, closeness centrality > 0.5371179), 48 nodes were identified as the key targets of WYJ against PF (Supplementary Table S4).

The 48 key targets obtained from PPI were selected to investigate the biological processes and mechanisms of WYJ on PF treatment. Results indicated that biological processes involve in PF treatment include positive regulation of transcription from RNA polymerase II promoter, signal transduction, etc. Pathway enrichment analyses using the KEGG database revealed that most of the therapeutic targets are associated with signal transduction (e.g., MAPK signaling pathway and PI3K-protein kinase B (Akt) signaling pathway), inflammation (e.g., TNF signaling pathway and HIF-1 signaling pathway) and immune response (e.g., Toll-like receptor signaling pathway and Jak-STAT signaling pathway). The disease is caused by basic biological dysfunction, so the KEGG pathway about human disease were deleted. 20 significant BP terms and KEGG pathway terms were shown in Fig. 4.

Compound–target-pathway network explored the connections of important compounds of WYJ, key targets, and top 20 related pathways. The integrated compound–target-pathway network visualized by Cytoscape consisted of 69 nodes and 258 edges (Fig. 5). STAT3, SRC, IL6, MAPK1, AKT1, EGFR, MAPK8, MAPK14 and IL1B were the nine most important nodes in the compound–target-pathway network based on comparing betweenness centrality, closeness centrality and degree (Supplementary Table S5). These nodes also interacted closely with MAPK signaling pathway(MAPK8, IL1B, MAPK1, AKT1, PRKCA, MAPK14, RELA, EGFR)in the KEGG results. These results indicated that WYJ relieves PF mainly via the MAPK signaling pathway. Interestingly, we also found that STAT3 is the top node in the compound–target-pathway network and involved in multiple pathways. Above, these results demonstrated that WYJ worked in PF treatment through overall cooperation with multiple pathways and multiple targets.

Molecular Docking

In this paper, molecular docking using AutoDock Vina was applied to verify the reliability of the results of network pharmacology. The association between 13 active compounds in WYJ and target genes was visualized by compound–target-pathway network. Considering the results of KEGG and compound–target-pathway network. Therefore, we explored the interactions between 13 key compounds and nine important targets (STAT3, SRC, IL6, MAPK1, AKT1, EGFR, MAPK8, MAPK14, IL1B). Docking and binding affinity of ligands into the binding site of receptors are important information for prediction of pharmacology[22]. Results showed that most of the ligands have good binding activity with receptors (Vina scores less than − 5 kcal/mol). The Vina scores were shown in Supplementary Table S6. The predicted target-compound with the highest affinity was visualized using PyMOL (Fig. 6).

Experimental verification of WYJ effects on the idiopathic pulmonary fibrosis

WYJ alleviated BLM-induced pulmonary fibrosis in mice

21 days after BLM injection, significant decreases in survival rate, severe weight loss and increase lung/body weight ratio were shown in BLM-induced PF model compared with the Control group. The WYJ treatment increased the survival rate, attenuated weight loss, and reduced the lung/body weight ratio (Fig. 7A, B, C). Hydroxyproline level, an important fibrotic indicator of collagen deposition, also decreased by the WYJ treatment (Fig. 7D). TGF-β1 is the important fibrotic factor in the development of pulmonary fibrosis[23, 24]. In our study, WYJ treatment down-regulated increased lung tissue TGF-β1 mRNA in PF mice model (Fig. 7E). BLM-induced PF mice model showed typical features of lung fibrosis, and WYJ prevented the development of lung fibrosis, as revealed by Masson staining (Fig. 7F) and Histopathological examination of lung sections (Fig. 7G). Above results confirmed that WYJ exerted a protective effect on lung fibrosis.

Excessive deposition of extracellular matrix (ECM), such as collagen[25], is the feature of fibrosis. The WYJ groups inhibited mRNA expression of Collagen-1 compared with the Model group (Fig. 8A). Fibroblasts lose their marker E-cadherin and transform to myofibroblasts characterized with α-SMA[24], occurs in the PF. As shown in Fig. 8B, bolts indicated the decreased α-SMA expression after the WYJ treatment compared with the Model group, indicating that the fibrosis process was inhibited by the WYJ treatment.

According to the network pharmacology analysis results, we assumed that MAPK signaling pathway could be the pharmacological mechanism of the therapeutic effect of WYJ against PF. Phosphorylation levels of MAPK1 (p-MAPK1) was increased in the Model group compared with the Control group (Fig. 8C). The WYJ treatment reduced the upregulation of p-MAPK1 expression in BLM-induced PF model.

Network pharmacology analysis showed that STAT3 is the top node in the compound–target-pathway network and involved in multiple pathways. Studies showed STAT3 is the common downstream target of fibrotic factors. Levels of phosphorylated STAT3 (p-STAT3) was elevated in the Model group. We detected that the WYJ treatment remarkably reduced the increased p-STAT3 (Fig. 8D). Pulmonary fibrosis is the result of multiple cytokines or signal transduction pathways. WYJ reduced pulmonary fibrosis by down-regulating p-STAT3, which may be a new perspective to explain anti-lung fibrosis of WYJ.

WYJ inhibited fibroblast activation in vitro experiments

In vitro experiments further verified the anti-lung fibrosis effect of WYJ. CCK-8 assay was used to determine the effect of WYJ on HPF activity. As shown in Fig. 9A, WYJ shows no effect on the viability of normal cells at 1–20 ng/ml. Activated lung fibroblasts, the primary roles in the progress of fibrogenesis, express excessive α-SMA and Collagen-1. To determine whether WYJ inhibits fibroblast activation, we used TGF-β1 to promote fibroblast activation[24] and evaluated the expression of α-SMA and collagen-1. The results demonstrated that HPF stimulated with TGF-β1 significantly increased the production of α-SMA (Fig. 9B) and Collagen-1 (Fig. 9C) protein. HPF pretreated with WYJ markedly inhibited expression of α-SMA and

Collagen-1 protein. And results also showed that WYJ prevented the activation of fibroblasts by down-regulating p-MAPK1 and p-STAT3 in vitro (Fig. 9D, E).

Discussion

TCMs has accumulated valuable information alleviating lung diseases. WYJ, from steamed roots of Curcuma wenyujin, was included in the 2020 edition of the Pharmacopoeia of People s Republic of China. Modern pharmacological studies have demonstrated that the ingredients or extracts from WYJ have antibacterial, antitumor anti-inflammatory and antioxidant[26] effects. There are studies reported that curcumin, an essential ingredient of WYJ, have anti-pulmonary fibrosis in murine model[27, 28]. Hui's study showed potential anti-fibrotic effects of WYJ in liver fibrosis[29]. In our present study, we investigated the effect of WYJ against PF and the related molecular mechanism.

In this study, we established PF mice model by administering (via the trachea) bleomycin at a dose of 5 mg/kg. This model could cause a pulmonary pathological change similar to that of patients with lung fibrosis[30, 31]. We explored the effect of WYJ on PF from the perspectives of the survival rate, HYP, and histopathological examination. In our study, three dosage groups of WYJ were evaluated. The results showed that all dosage groups hindered lung fibrosis, and the WYJ-H and WYJ-M groups demonstrated the best therapeutic effect.

We identified 23 major compounds from WYJ using UHPLC-LTQ-Orbitrap. Further the network pharmacology results revealed that 128 targets could be potential targets on the treatment of PF, and PPI network showed 48 of them were key targets. KEGG analysis results and the compound–target-pathway network suggested that STAT3, SRC, IL6, MAPK1, AKT1, EGFR, MAPK8, MAPK14 and IL1B are important targets. MAPK8, MAPK1, AKT1, MAPK14, EGFR and IL1B were the important targets in MAPK signaling pathway. STAT3 was the top node in the compound–target-pathway network and involved in multiple pathways. The prediction results indicated that WYJ relieved pulmonary fibrosis mainly through inhibiting the MAPK signaling pathway and down-regulating the expression of p-STAT3.

MAPKs signaling cascades participate in the regulation of processes including cell cycle progression, cell migration, cell survival and differentiation[32, 33]. Katerina M and colleagues[34] found BRAF,a major signaling intermediate protein that regulates the MAPK/ERK pathway increased in lung tissue of patients with IPF compared with normal. Another study found activated MAPKs are significantly increased in lung parenchyma of patients with IPF compared that of normal[35]. Bach1 ameliorated fibrosis and inflammation via blocking MAPK pathway in pulmonary fibrosis in recent study[36]. Another study proved that the blockade of ERK by PD98059 attenuated the increase of collagen mRNA expression induced by TGF-β1[37]. In our study, the WYJ treatment remarkably reduced the increased α-SMA, Collagen-1, and levels of p-MAPK1 in BLM-induced PF model and TGF-β1 induced HPF cells. The inhibitory effect of WYJ on PF may function mainly through modulating the MAPK signaling pathway.

Compound–target-pathway network revealed that STAT3 is the top node in PF treatment with WYJ. STAT3 regulates cell growth, proliferation, differentiation, and migration.[38] Important fibrotic factors including TGF-β1, PDGF, FGF-2, and IL-13 can activate STAT3[39–43] and further lead to pulmonary fibrosis. Levels of phosphorylated STAT3 have been shown to be elevated in patients with IPF and bleomycin model[44–47]. C-188-9[42], a synthetic small molecule inhibitor of STAT3 phosphorylation, inhibited STAT3 activation and decreased the development of pulmonary fibrosis in BLM-induced PF model. Accordingly, targeting common downstream mediators of fibrogenic mediators, STAT3, PF can be treated by several of the cellular pathways. In our study, elevated levels of p-STAT3 were observed in BLM-induced PF model and TGF-β1 induced HPF cells. The WYJ treatment remarkably reduced the increased p-STAT3. WYJ relieves pulmonary fibrosis by down-regulating the expression of P-STAT3.

We also explored the effect of WYJ on PF from another perspective using molecular docking. The results proved that compounds of WYJ have good binding activity with key targets (MAPK8, MAPK1, AKT1, MAPK14, EGFR, IL1B and STAT3), further illustrating that WYJ could hinder lung fibrosis via inhibiting the MAPK signaling pathway and down-regulating the expression of p-STAT3.

This study has some drawbacks. Compounds which have the most effective therapeutic effects require further definite and research. The network pharmacology had limitations. A total of 23 Compounds of WYJ were confirmed based on UHPLC-LTQ-Orbitrap. However, only targets of 15 Compounds were obtained from databases and the network pharmacology only involved targets of 13 Compounds. Whether the remaining Compounds play an anti-pulmonary fibrosis effect needs further research. The pharmacological mechanism by which WYJ treated PF need further exploration.

Conclusions

In conclusion, our study identified that WYJ alleviated pulmonary fibrosis (Fig. 10). According to the results of network pharmacology and molecular docking, the pharmacological mechanism by which WYJ-treated PF was further validated by experiment. The inhibitory effect of WYJ on PF may function mainly through modulating the MAPK signaling pathway. Interestingly, WYJ reduced pulmonary fibrosis by down-regulating p-STAT3, which may provide new insights for the treatment of WYJ on pulmonary fibrosis. The method of exploring the pharmacological mechanism of WYJ in our study provides a novel approach to explain the pharmacological basis of other herbs. The limitations of network pharmacology indicate that more experiments are needed to verify the reliability anti-fibrotic effect of WYJ.

Abbreviations

PF : Pulmonary fibrosis ;WYJ : Wen-yu-jin ; UHPLC-LTQ-orbital trap : Ultra-high pressure liquid chromatography combined with linear ion trap-orbital tandem mass spectrometry ;p-STAT3 : phosphorylated STAT3 ;p-MAPK1 : phosphorylated MAPK1 ;IPF : Idiopathic pulmonary fibrosis ;TCMs : Traditional Chinese Medicines ;PPI : protein-protein interaction ;GO : Gene Ontology ;KEGG : Kyoto Encyclopedia of Genes and Genomes ;BLM : bleomycin ;C : the Control group ;M : the Model group ; WYJ-H : bleomycin with WYJ high concentration treatment group ; WYJ-M : bleomycin with WYJ medium concentration treatment group ;WYJ-L : bleomycin with WYJ low concentration treatment group ;BW : body weight ;PW : whole lung weight ;PI : Pulmonary indexes ;HPF : Human pulmonary fibroblast; EMC: Excessive deposition of extracellular matrix .

Declarations

Ethics approval and consent to participate

Animal procedures were performed according to the protocols of Animal Care and Use Committee of Beijing University of Chinese Medicine.

Consent to publish

All authors have provided consent for publication in the Journal of Chinese Medicine.

Availability of data and materials

The datasets used and analyzed during the current study are available from the corresponding author on reasonable request.

Competing interests

The authors declare that they have no competing interests.

Funding

Not applicable.

Authors' Contributions

LW and WX-Z made substantial contributions to the conception and design of the study, performed the experiments and wrote the paper. RS, BB-Z and QH-M assisted in the performance of experiments. JL participated in data analysis. YY-S modified the experimental protocol, revised the manuscript, and finally approved the version to be published. All authors read and approved the final manuscript.

Acknowledgements

Not applicable.

References

1. Hochhegger B, Marchiori E, Zanon M, Rubin AS, Fragomeni R, Altmayer S, Carvalho CRR, Baldi BG, Imaging in idiopathic pulmonary fibrosis: diagnosis and mimics, Clinics (Sao Paulo, Brazil) 74 (2019) e225.
2. Meyer KC. Pulmonary fibrosis, part I: epidemiology, pathogenesis, and diagnosis. Expert Rev Respir Med. 2017;11(5):343–59.
3. Selman M, Pardo A. Revealing the pathogenic and aging-related mechanisms of the enigmatic idiopathic pulmonary fibrosis. an integral model. Am J Respir Crit Care Med. 2014;189(10):1161–72.
4. Martinez FJ, Collard HR, Pardo A, Raghu G, Richeldi L, Selman M, Swigris JJ, Taniguchi H, Wells AU. Idiopathic pulmonary fibrosis, Nature reviews. Disease primers. 2017;3:17074.
5. Cho SJ, Stout-Delgado HW. Aging Lung Disease Annual review of physiology. 2020;82:433–59.
6. Abramson MJ, Murambadoro T, Alif SM, Benke GP, Dharmage SC, Glaspole I, Hopkins P, Hoy RF, Klebe S, Moodley Y, Rawson S, Reynolds PN, Wolfe R, Corte TJ, Walters EH. Occupational and environmental risk factors for idiopathic pulmonary fibrosis in Australia: case-control study. Thorax. 2020;75(10):864–9.
7. Staitieh BS, Renzoni EA, Veeraraghavan S. Pharmacologic therapies for idiopathic pulmonary fibrosis, past and future. Annals of medicine. 2015;47(2):100–5.
8. Tzouvelekis A, Bonella F, Spagnolo P. Update on therapeutic management of idiopathic pulmonary fibrosis, Therapeutics and clinical risk management 11 (2015) 359–70.

9. Azuma A, Nukiwa T, Tsuboi E, Suga M, Abe S, Nakata K, Taguchi Y, Nagai S, Itoh H, Ohi M, Sato A, Kudoh S. Double-blind, placebo-controlled trial of pirfenidone in patients with idiopathic pulmonary fibrosis. Am J Respir Crit Care Med. 2005;171(9):1040–7.
10. Flaherty KR, Wells AU, Cottin V, Devaraj A, Walsh SLF, Inoue Y, Richeldi L, Kolb M, Tetzlaff K, Stowasser S, Coeck C, Clerisme-Beaty E, Rosenstock B, Quaresma M, Haeufel T, Goeldner RG, Schlenker-Herceg R, Brown KK. Nintedanib in Progressive Fibrosing Interstitial Lung Diseases. N Engl J Med. 2019;381(18):1718–27.
11. Ogura T, Kitamura H. Tolerability of treatment with pirfenidone or nintedanib for pulmonary fibrosis in the real world. Respirology. 2017;22(6):1051–2.
12. Rodríguez-Portal JA. Efficacy and Safety of Nintedanib for the Treatment of Idiopathic Pulmonary Fibrosis: An Update. Drugs R D. 2018;18(1):19–25.
13. Li LC, Kan LD. Traditional Chinese medicine for pulmonary fibrosis therapy: Progress and future prospects. J Ethnopharmacol. 2017;198:45–63.
14. Daina A, Michielin O, Zoete V. SwissTargetPrediction: updated data and new features for efficient prediction of protein targets of small molecules. Nucleic acids research. 2019;47(W1):W357-w364.
15. Stelzer G, Rosen N, Plaschkes I, Zimmerman S, Twik M, Fishilevich S, Stein TI, Nudel R, Lieder I, Mazor Y, Kaplan S, Dahary D, Warshawsky D, Guan-Golan Y, Kohn A, Rappaport N, Safran M, Lancet D, The GeneCards Suite: From Gene Data Mining to Disease Genome Sequence Analyses, Current protocols in bioinformatics 54 (2016) 1.30.1–1.30.33.
16. Amberger JS, Bocchini CA, Schiettecatte F, Scott AF, Hamosh A. OMIM.org: Online Mendelian Inheritance in Man (OMIM®), an online catalog of human genes and genetic disorders, Nucleic acids research 43(Database issue) (2015) D789-98.
17. Szklarczyk D, Gable AL, Nastou KC, Lyon D, Kirsch R, Pyysalo S, Doncheva NT, Legeay M, Fang T, Bork P, Jensen LJ, von Mering C. The STRING database in 2021: customizable protein-protein networks, and functional characterization of user-uploaded gene/measurement sets. Nucleic acids research. 2021;49(D1):D605-d612.
18. Dennis G Jr, Sherman BT, Hosack DA, Yang J, Gao W, Lane HC, Lempicki RA. DAVID: Database for Annotation, Visualization, and Integrated Discovery. Genome biology. 2003;4(5):P3.
19. Huang da W, Sherman BT, Lempicki RA. Bioinformatics enrichment tools: paths toward the comprehensive functional analysis of large gene lists. Nucleic acids research. 2009;37(1):1–13.
20. Trott O, Olson AJ. AutoDock Vina: improving the speed and accuracy of docking with a new scoring function, efficient optimization, and multithreading. J Comput Chem. 2010;31(2):455–61.
21. Seeliger D, de Groot BL. Ligand docking and binding site analysis with PyMOL and Autodock/Vina. J Comput Aided Mol Des. 2010;24(5):417–22.
22. Pinzi L, Rastelli G. Molecular Docking: Shifting Paradigms in Drug Discovery, International journal of molecular sciences 20(18) (2019).
23. Ask K, Bonniaud P, Maass K, Eickelberg O, Margetts PJ, Warburton D, Groffen J, Gauldie J, Kolb M. Progressive pulmonary fibrosis is mediated by TGF-beta isoform 1 but not TGF-beta3. Int J Biochem Cell Biol. 2008;40(3):484–95.
24. Thannickal VJ, Lee DY, White ES, Cui Z, Larios JM, Chacon R, Horowitz JC, Day RM, Thomas PE. Myofibroblast differentiation by transforming growth factor-beta1 is dependent on cell adhesion and integrin signaling via focal adhesion kinase. J Biol Chem. 2003;278(14):12384–9.
25. Pardo A, Selman M, Matrix metalloproteases in aberrant fibrotic tissue remodeling, Proceedings of the American Thoracic Society 3(4) (2006) 383-8.
26. Yin GP, Zhang QZ, An YW, Zhu JJ, Wang ZM. [Advance in chemical constituents and pharmacological activity of Curcuma wenyujin], Zhongguo Zhong yao za zhi = Zhongguo zhongyao zazhi = China. journal of Chinese materia medica. 2012;37(22):3354–60.
27. Cho YJ, Yi CO, Jeon BT, Jeong YY, Kang GM, Lee JE, Roh GS, Lee JD. Curcumin attenuates radiation-induced inflammation and fibrosis in rat lungs, The Korean journal of physiology & pharmacology: official journal of the Korean Physiological Society and the Korean Society of Pharmacology 17(4) (2013) 267 – 74.
28. Lee JC, Kinniry PA, Arguiri E, Serota M, Kanterakis S, Chatterjee S, Solomides CC, Javvadi P, Koumenis C, Cengel KA, Christofidou-Solomidou M. Dietary curcumin increases antioxidant defenses in lung, ameliorates radiation-induced pulmonary fibrosis, and improves survival in mice. Radiation research. 2010;173(5):590–601.
29. Xie H, Su D, Zhang J, Ji D, Mao J, Hao M, Wang Q, Yu M, Mao C, Lu T. Raw and vinegar processed Curcuma wenyujin regulates hepatic fibrosis via bloking TGF-β/Smad signaling pathways and up-regulation of MMP-2/TIMP-1 ratio. J Ethnopharmacol. 2020;246:111768.
30. Border WA, Noble NA. Transforming growth factor beta in tissue fibrosis. N Engl J Med. 1994;331(19):1286–92.
31. Della Latta V, Cecchettini A, Del Ry S, Morales MA. Bleomycin in the setting of lung fibrosis induction: From biological mechanisms to counteractions. Pharmacological research. 2015;97:122–30.
32. Morrison DK. MAP kinase pathways, Cold Spring Harbor perspectives in biology 4(11) (2012).
33. Roskoski R Jr. ERK1/2 MAP kinases: structure, function, and regulation. Pharmacological research. 2012;66(2):105–43.
34. Antoniou KM, Margaritopoulos GA, Soufla G, Symvoulakis E, Vassalou E, Lymbouridou R, Samara KD, Kappou D, Spandidos DA, Siafakas NM. Expression analysis of Akt and MAPK signaling pathways in lung tissue of patients with idiopathic pulmonary fibrosis (IPF). J Recept Signal Transduct Res. 2010;30(4):262–9.

35. Yoshida K, Kuwano K, Hagimoto N, Watanabe K, Matsuba T, Fujita M, Inoshima I, Hara N. MAP kinase activation and apoptosis in lung tissues from patients with idiopathic pulmonary fibrosis. J Pathol. 2002;198(3):388–96.
36. Liu Y, Wang Y, Lu F, Wang L, Miao L, Wang X. BTB and CNC homology 1 inhibition ameliorates fibrosis and inflammation via blocking ERK pathway in pulmonary fibrosis. Experimental lung research. 2021;47(2):67–77.
37. Hung KY, Chen CT, Huang JW, Lee PH, Tsai TJ, Hsieh BS. Dipyridamole inhibits TGF-beta-induced collagen gene expression in human peritoneal mesothelial cells. Kidney international. 2001;60(4):1249–57.
38. Levy DE, Darnell JE Jr. Stats: transcriptional control and biological impact, Nature reviews. Molecular cell biology. 2002;3(9):651–62.
39. Chakraborty D, Šumová B, Mallano T, Chen CW, Distler A, Bergmann C, Ludolph I, Horch RE, Gelse K, Ramming A, Distler O, Schett G, Šenolt L, Distler JHW. Activation of STAT3 integrates common profibrotic pathways to promote fibroblast activation and tissue fibrosis. Nature communications. 2017;8(1):1130.
40. Bagnato G, Harari S. Cellular interactions in the pathogenesis of interstitial lung diseases. European respiratory review: an official journal of the European Respiratory Society. 2015;24(135):102–14.
41. Ogata H, Chinen T, Yoshida T, Kinjyo I, Takaesu G, Shiraishi H, Iida M, Kobayashi T, Yoshimura A. Loss of SOCS3 in the liver promotes fibrosis by enhancing STAT3-mediated TGF-beta1 production. Oncogene. 2006;25(17):2520–30.
42. Pedroza M, Le TT, Lewis K, Karmouty-Quintana H, To S, George AT, Blackburn MR, Tweardy DJ, Agarwal SK. STAT-3 contributes to pulmonary fibrosis through epithelial injury and fibroblast-myofibroblast differentiation, FASEB journal: official publication of the Federation of American Societies for. Experimental Biology. 2016;30(1):129–40.
43. Wolters PJ, Collard HR, Jones KD. Pathogenesis of idiopathic pulmonary fibrosis, Annual review of pathology 9 (2014) 157 – 79.
44. Le TT, Karmouty-Quintana H, Melicoff E, Le TT, Weng T, Chen NY, Pedroza M, Zhou Y, Davies J, Philip K, Molina J, Luo F, George AT, Garcia-Morales LJ, Bunge RR, Bruckner BA, Loebe M, Seethamraju H, Agarwal SK, Blackburn MR, Blockade of IL-6 Trans signaling attenuates pulmonary fibrosis, Journal of immunology (Baltimore, Md.: 1950) 193(7) (2014) 3755-68.
45. Moodley YP, Scaffidi AK, Misso NL, Keerthisingam C, McAnulty RJ, Laurent GJ, Mutsaers SE, Thompson PJ, Knight DA. Fibroblasts isolated from normal lungs and those with idiopathic pulmonary fibrosis differ in interleukin-6/gp130-mediated cell signaling and proliferation, The American journal of pathology 163(1) (2003) 345 – 54.
46. O'Donoghue RJ, Knight DA, Richards CD, Prêle CM, Lau HL, Jarnicki AG, Jones J, Bozinovski S, Vlahos R, Thiem S, McKenzie BS, Wang B, Stumbles P, Laurent GJ, McAnulty RJ, Rose-John S, Zhu HJ, Anderson GP, Ernst MR, Mutsaers SE. Genetic partitioning of interleukin-6 signalling in mice dissociates Stat3 from Smad3-mediated lung fibrosis, EMBO molecular medicine 4(9) (2012) 939 – 51.
47. Pechkovsky DV, Prêle CM, Wong J, Hogaboam CM, McAnulty RJ, Laurent GJ, Zhang SS, Selman M, Mutsaers SE, Knight DA. STAT3-mediated signaling dysregulates lung fibroblast-myofibroblast activation and differentiation in UIP/IPF. Am J Pathol. 2012;180(4):1398–412.

Figures

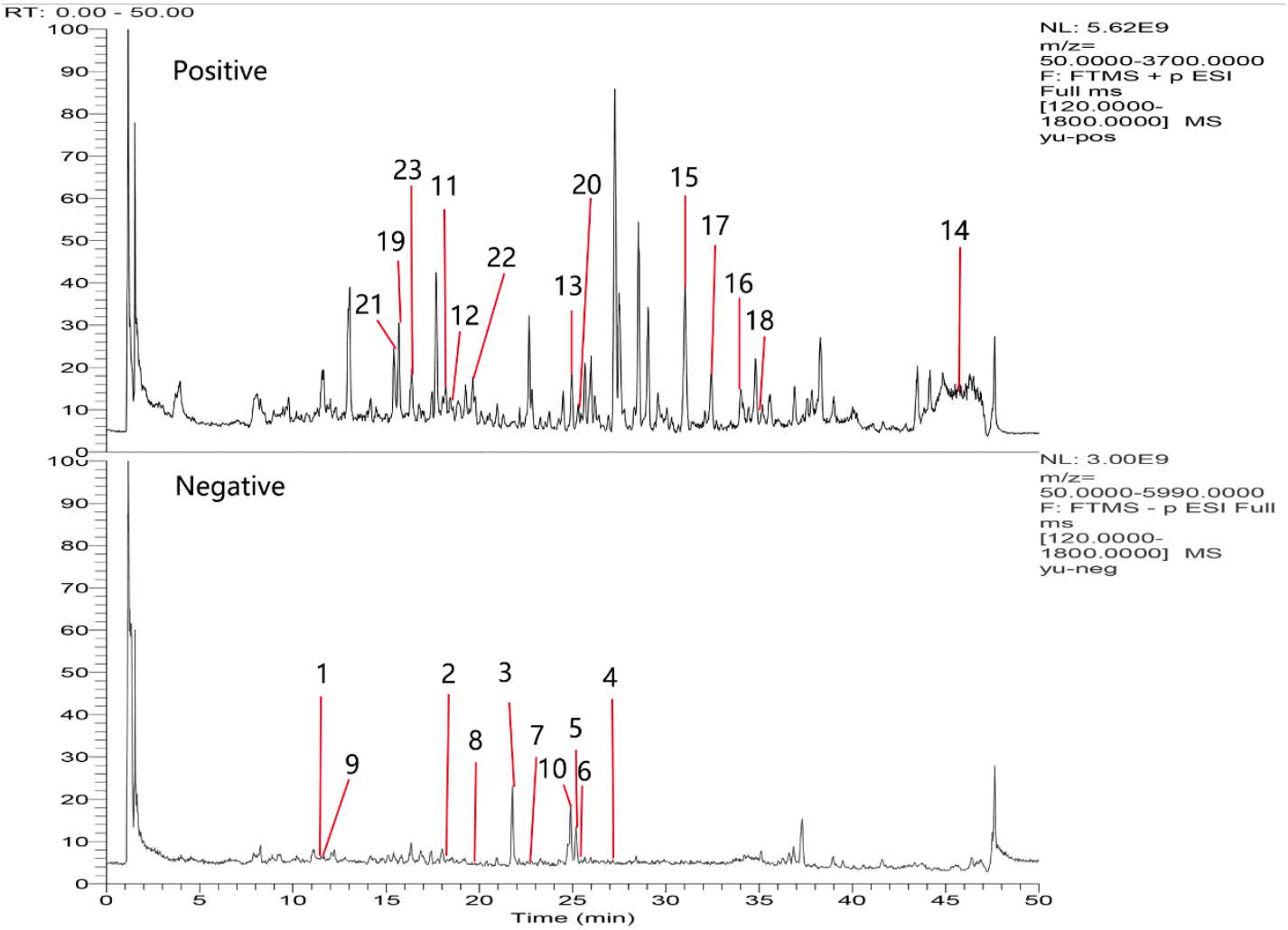

Figure 1

Total ion chromatogr

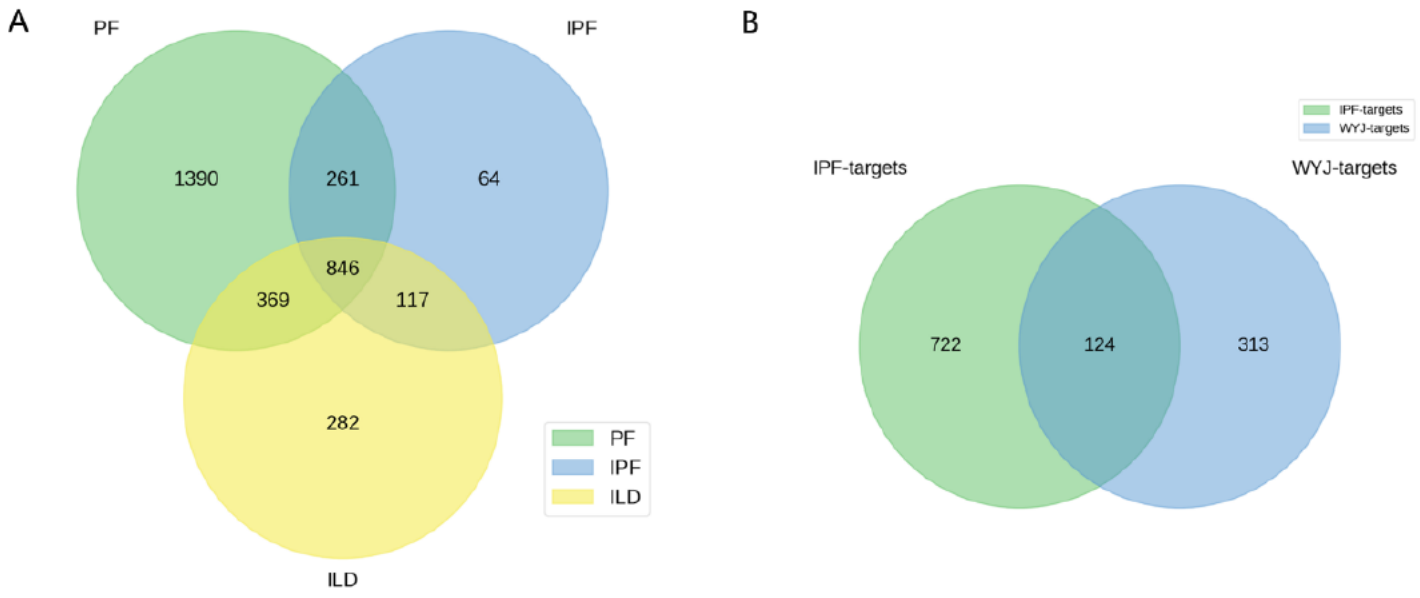

Figure 2

(A) Venn diagram of IPF-related targets. (B) Venn diagram of potential targets for WYJ treatment on PF.

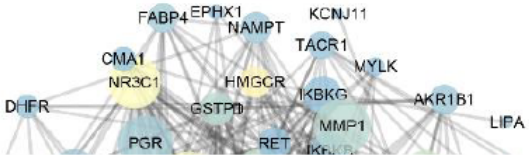

Figure 3

PPI network of potential targets.

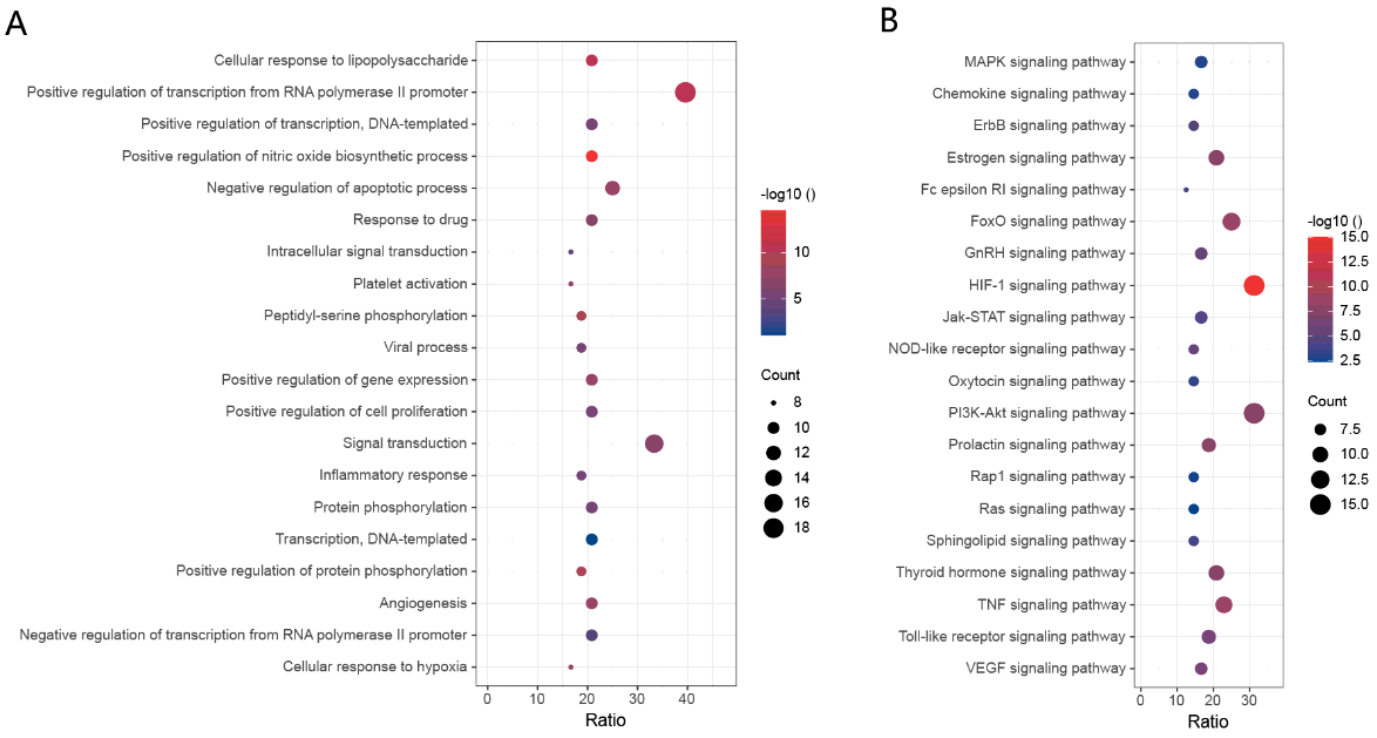

Figure 4

Bubble diagram of functional analysis. (A) Enrichment analysis of biological process (B) KEGG pathway enrichment analysis.

Figure 5

The integrated compound–target-pathway network visualized by Cytoscape.

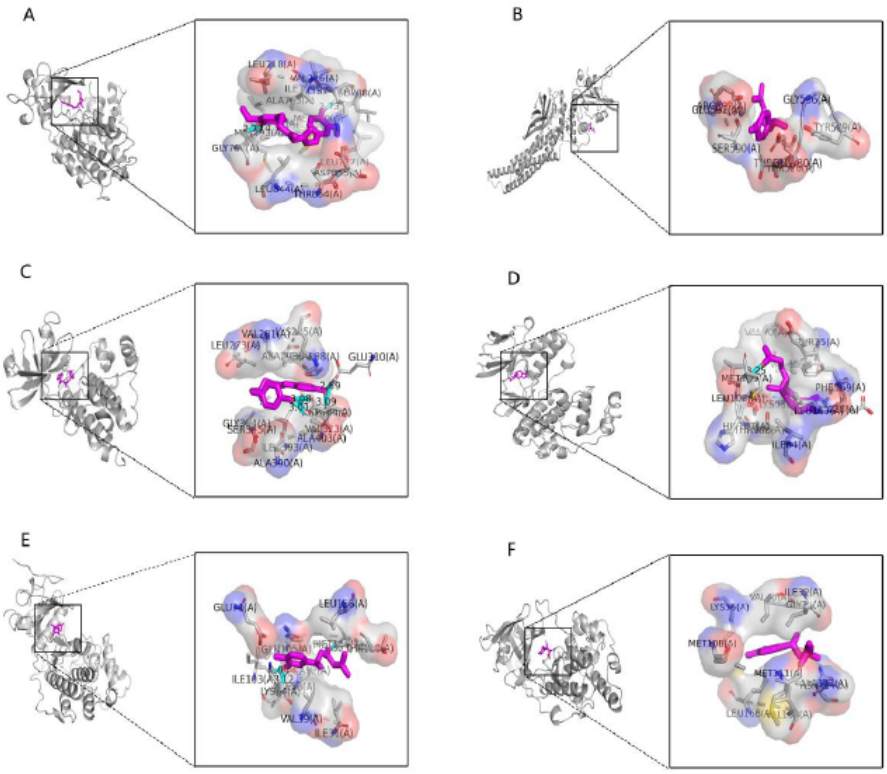

Figure 6

The binding modes of ligand and receptor protein. (A) Schematic diagram of the interplay between 1,2-Dihydrocurcumin and EGFR (PDB IDchimeric 5YU9). (B) Schematic diagram of the interplay between ar-turmerone and STAT3 (PDB IDchimeric 6TLC). (C) Schematic diagram of the interplay between bisdemethoxycurcumin and SRC (PDB IDchimeric 2BDF). (D) Schematic diagram of the interplay between Curcumenolactone A and MAPK14 (PDB IDchimeric 1SFO). (E) Schematic diagram of the interplay between turmeronol A and MAPK1 (PDB IDchimeric 1TVO). (F) Schematic diagram of the interplay between turmeronol A and MAPK8 (PDB IDchimeric 3ELJ).

Figure 7

WYJ alleviated BLM-induced pulmonary fibrosis in mice. (A) Survival rate. (B) The body weight. (C) Lung/Body weight ratio. (D) Hydroxyproline. (E) Lung tissue TGF-β1 mRNA. (F) The representative images of Masson staining. (G) The representative images of H&E staining. C: The Control group. M: The Model group. The data were presented as mean ± SEM (n≥3). *P< 0.05, **P< 0.01 and ***P< 0.001 versus the Model group; #P< 0.05, ##P< 0.01 and ###P< 0.001 versus the control group

Figure 8

The effect of WYJ on BLM-induced pulmonary fibrosis mice. (A) mRNA expressions of Collagen-1 in lung tissues were measured by qRT-PCR. (B-D) The relative protein levels of α-SMA, p-MAPK1 and p-STAT3. C: The Control group. M: The Model group. The data were presented as mean ± SEM (n≥3). *P< 0.05, **P< 0.01 and ***P< 0.001 versus the Model group; #P< 0.05, ##P< 0.01 and ###P< 0.001 versus the control group

Figure 9

(A)The effect of WYJ on HPF activity. (B-E) The relative protein levels of α-SMA, Collagen-1, p-MAPK1 and p-STAT3. C: The Control group. M: The Model group. The data were presented as mean ± SEM (n≥3). *P< 0.05, **P< 0.01 and ***P< 0.001 versus the Model group; #P< 0.05, ##P< 0.01 and ###P< 0.001 versus the control group

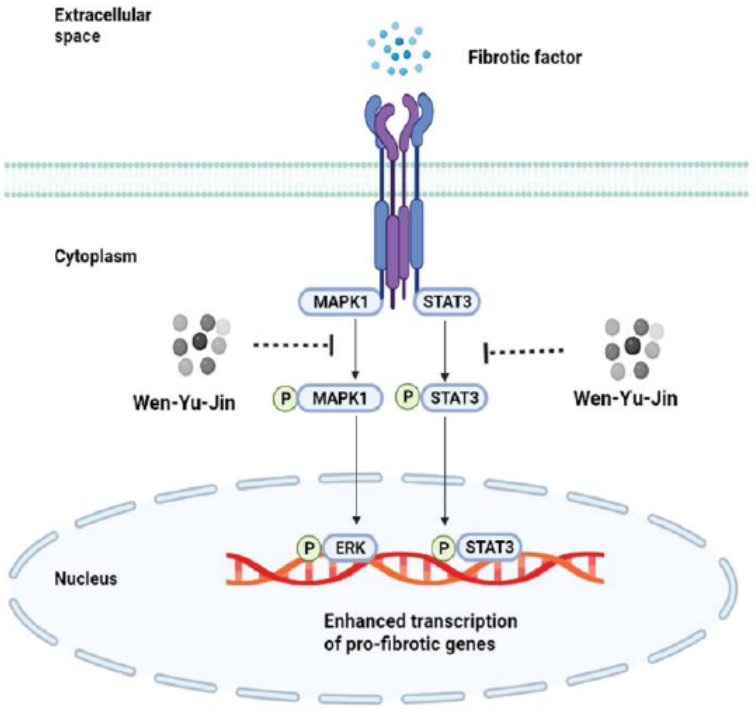

Figure 10

The underlying mechanisms involved in the anti-lung fibrotic activity of WYJ.

Supplementary Files

This is a list of supplementary files associated with this preprint. Click to download.

- SupplementaryTable.xlsx